**Iraqi Geological Journal**

Journal homepage: https://www.igj-iraq.org

# Determination of Petrophysical Parameters using Well Logs for Mishrif Formation in F Oil Field Southern Iraq

**Madyan H. Ali[1,*], Rafid N. Rajab[1] and Mahmood J. Al-Khafaji[2]**

[1] Department of Geology, College of Science, University of Basra, Basra, Iraq
[2] Missan Oil Company, Missan, Iraq
* **Correspondence**: mdnhdi@gmail.com

Received:
30 December 2021

Accepted:
15 February 2022

Published:
30 April 2022

## Abstract

This research aims to identify and analyze the Mishrif Formation's reservoir units and subunits in the F oilfield, located north of the Nasiriya using mostly well-logging data and other accessible geological data. The Petrophysical and lithological parameters of each unit of the Mishrif Formation are determined using data from the F-X1, F-X2, and F-X3 wells to evaluate the water saturation for each unit. GEOLOG8 software was used to interpret output data. High reservoir potential is found in units M1.2, L1.1, L1.2 and L2 due to the high effective porosity and low water saturation. The reservoir units are separated by cap units including marl key beds and units M1.1, M2.

**Keywords:** Mishrif Formation; F oil field; Petrophysical parameters

## 1. Introduction

The Mishrif Formation consists of major carbonate reservoirs in southeast Iraq, with 32 structures containing oil (Awadeesian et al., 2019). The oilfields of Rumaila, West Qurna, Zubair fields, Majnoon, and Halfaiya have the largest both oil accumulation and large-scale north-south trending anticline structures. Other commercial oil accumulations in the Mishrif Formation found in Abu Ghirab, Ahdab, Amara, Buzurgan, Dujaila, Gharraf, Hawaiza, and Jabel Fauqi (Aqrawi et al., 2010).

Due to its economic hydrocarbon accumulations, several studies have been conducted for the Mishrif Formation in Southern Iraq. These studies involve different disciplines including stratigraphy and petrophysics. For example, microfacies were used to interpret the environment of depositional and diagenetic processes of the Mishrif Formation in the Nassyriah (Handhal and Al-Shahwan, 2014), Faiha and Sindibad oil fields (Handhal et al., 2020). Facies analysis studies combine microfacies data with image logsdies (Ismail et al., 2021). Petrophysical studies include estimating the values of porosity and permeability by using conventional logs and nuclear magnetic resonance log (NMR) of the Mishrif formation as in the Buzurgan oil field (Al-Janaee and Al-shahwan, 2019). In addition, the output of well logs analysis was used in reservoir modeling of petrophysical properties in many oil fields as in Noor (Al-Najm et al., 2017), Tuba (Mohammed and Mahdi, 2019), and Majnoon (Abbas and Mahdi, 2020). The characterization of the reservoir and non-reservoir units of the Mishrif Formation were carried out by using different approaches, including geochemical and geophysical interpretation (Al-Mimar et al., 2018), chronostratigraphic-based facies distribution (Awadeesian et al., 2018), brine chemistry (Awadh, et al., 2018). Paleontological and paleoecological studies have been limited to foraminifera and rudists

DOI: 10.46717/igj.55.1D.5Ms-2022-04-21

(Al-Dulaimy and Al-Sheikhly, 2013; Al-Dulaimi et al., 2013). F oilfield produces commercial hydrocarbons from the Mishrif Formation, and it was chosen for this study. The Mishrif Formation in F oilfield was first investigated as part of an Exploration Oil Company, geological-reservoir study in 1988 , and it was discovered that the Formation is made up of three main units: upper, middle, and lower units (South Oil Company, 1991).

## 2. Location and Geological Setting of the study Area

The F field is situated in the South of Iraq, in the Thi Qar Governorate (Fig.1). It was discovered between 1976 and 1978. The main reservoirs are discovered in Mishrif and Yamama formations. Less important oil accumulations are found in Ratawi and Zubair formations (Oil Exploration Company, 1995) (Fig. 2). The surface geology of the study area is characterized by flood plain sediments consisting of clay, sand and sediments of marshes and swamps of the modern Quaternary era (Oil Exploration Company, 2010). In F oil field, 116 wells have been drilled since 1983. Two vertical wells (F-X1, F-X2) and one directional well (F-X3) were chosen for this study (Table, 1) (Fig. 3).


**Fig.1.** Location map of F field

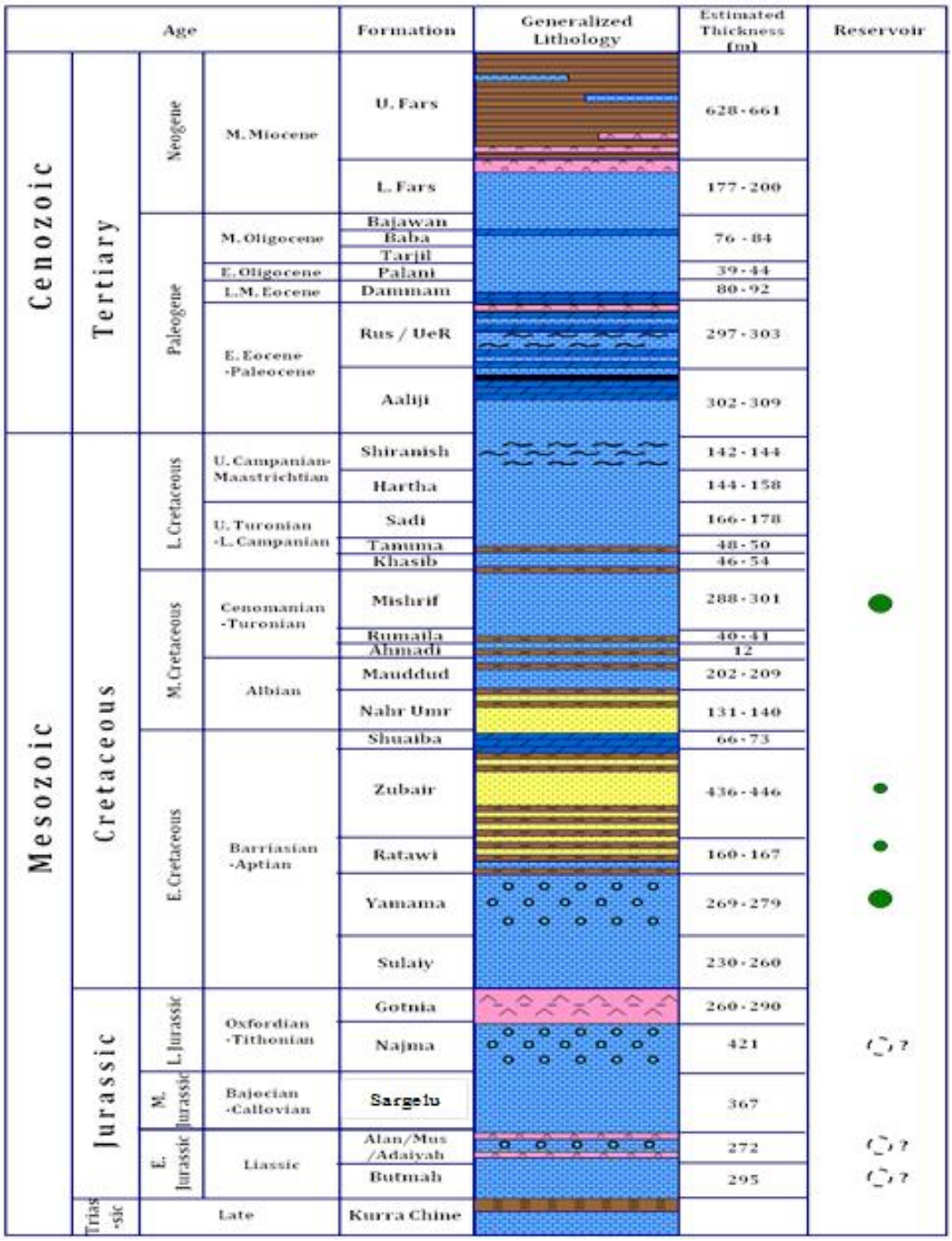


**Fig.2.** Stratigraphic column of the F oil field based on observation from F-1, F-2 and F-3 combined with F-X1 wells.

**Table 1.** Information of the studied wells

| Well ID | Well types | Well Trajectory | Top of Mishrif Fm. (mMD) |
|---|---|---|---|
| F-X1 | Appraisal | Vertical | 2245.5 |
| F-X2 | Development | Vertical | 2259.6 |
| F-X3 | Development | S shape Deviated | 3076.1 |

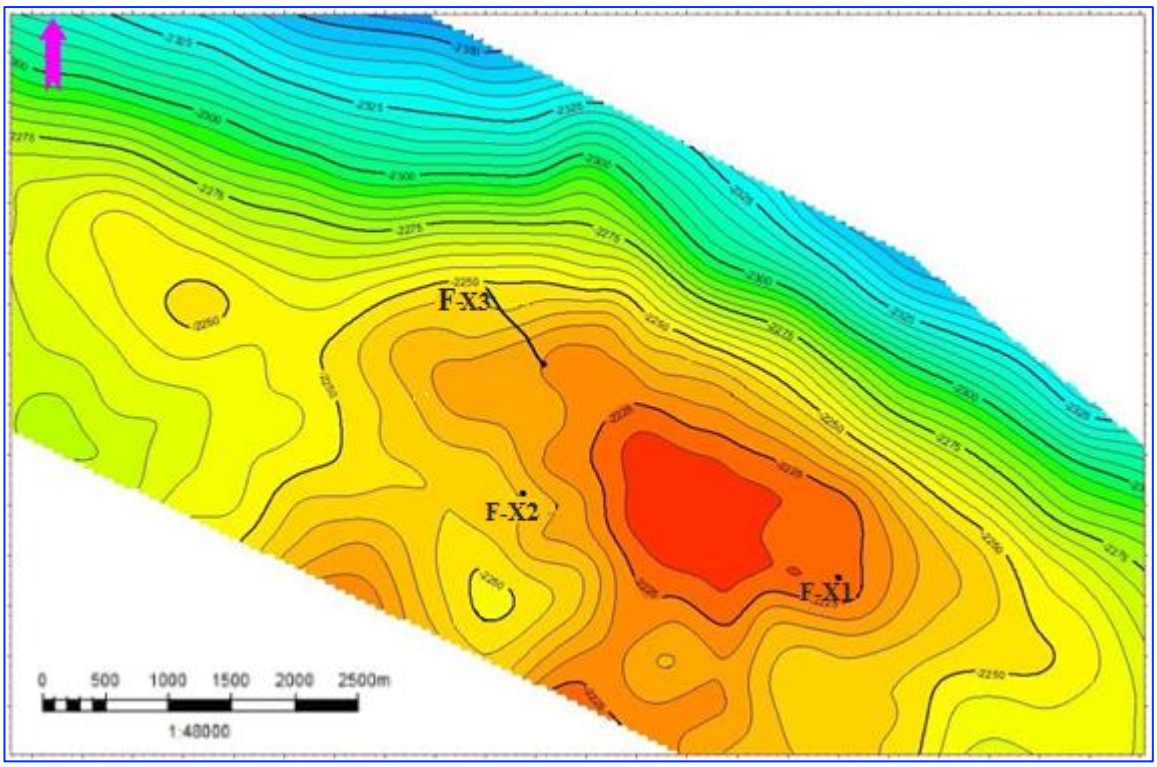


**Fig.3.** Top Mishrif depth structure map shows location of study wells

## 3. Aims of the study

The objectives of this research include analysis and interpretation of well logs data to predict and calculate the Petrophysical parameters such as porosity and water saturation.

## 4. Materials and Methods

The methodology of this research consists of the following:

- The accessible open hole logs data was digitized so that they could be transferred into the proper program for analysis it and interpretation. The logs were digitized using Didger V.3.02 software. The input data was interpolated to be in 0.5m sampling rate. The proper environmental correction (effect of Shale, conditions of borehole, invasion depth, etc.) were applied before determining the Petrophysical parameters from Neutron, gamma ray, resistivity and density logs.
- (Paradigm Geology) well log analysis software was used to determine petrophysical parameters include of water resistivity (Rw), lithology, shale volume, porosity (total and effective), water saturation, oil volume, and produce Computer Processed Interpretation (CPI) for each well.

## 5. Petrophysical Properties

Petrophysical characteristics must be determined and assessed in order to infer reservoir properties of the Mishrif formation as following:

### 5.1. Shale Volume (Vsh)

To derive Shale volume (Vsh) from the Gamma ray log (GR), the index of gamma ray (IGR) must be calculated using the following equation (Schlumberger, 1974):

$$IGR=(GRlog - GRmin)/(GRmax - GRmin), \quad (1)$$

where: IGR = Index of gamma ray, GR log= Reading of gamma ray by log (API); GR min= minimum of gamma ray (clean carbonate or sand); GR max= maximum of gamma ray (shale). And the following Dresser formula (Dresser, 1979) used to calculate the volume of shale:

$$Vsh=0.33\times(2^{2\times GIR} - 1), \quad (2)$$

High values of shale volume are observed at the top of Mishrif formation which is a clear indicator on gamma ray log whom used as a marker for top of Mishrif formation. The other major zone of high shale volume is the Marl unite. The Marl unite is the cap rock of the reservoir separating the non-reservoir upper Mishrif unites (U1, U2) from the reservoir unites of middle and lower Mishrif unites (M1.2, L1.1, L1.2 and L2).

### 5.2. Porosity(Ø)

The total porosity of the Mishrif Formation was calculated by using of the Neutron-Density logs. The Neutron porosity was corrected of shale effect using equation 3 (Tiab and Donaldson, 1996):

$$\varphi Ncorr = \varphi N - (Vsh \times \varphi Nsh), \quad (3)$$

where: φNcorr = shale effect corrected neutron porosity (fraction); $\varphi$N= raw neutron porosity (fraction); Vsh= shale volume of gamma ray (fraction); φNsh = Neutron porosity of shale (fraction).

Density derived porosity was determine using equation(4) (Wyllie, Gregory and Gardner, 1958):

$$ØD = (\rho ma - \rho b)/(\rho ma - \rho f), \quad (4)$$

where: ØD = shale effect corrected density derived porosity (fraction); $\rho$ma = density of matrix (2.71 gm/cm3) for limestone, (2.87 gm/cm3) for dolomite; $\rho$b = formation bulk density recorded by density log (g/cm3); $\rho$f = fluid Density (mud filtrate) (1g/cm3) for fresh water or (1.1 g/cm3) for salt mud. Density derived porosity although was corrected of shale effect using the following equation to remove the effect of shale from the calculation of porosity in intervals with a shale volume more than 10%:

$$\varphi Dcorr = \varphi D - (Vsh \times \varphi Dsh), \quad (5)$$

where: φNcorr = shale effect corrected density derived porosity (fraction); φD= raw density derived porosity (fraction); Vsh= shale volume of gamma ray (fraction); φDsh=Density derived porosity for shale (fraction).

Total porosity (φt) computed from density-neutron porosities as following:

$$\varphi t = (\varphi N + \varphi D)/2, \quad (6)$$

Effective porosity (φe) was computed by removing the shale-related pores from the total rock pores network using equation (7) (Schlumberger, 1998):

$$\varphi e = \varphi t \times (1 - Vsh), \quad (7)$$

where: φe = effective porosity; φt = total porosity; Vsh = volume of shale.

At the study wells, high values of porosity (total and effective) are observed in the middle and lower unites of Mishrif formation (M and L), that indicates of good hydrocarbon storage capacity reservoir as Table 2. Maximum porosity values are observed in M1.2, L1.1, L1.2 units that occur at the middle and lower parts of the Mishrif Fm. as reservoirs beds, and can be distinguished in all studied wells.

Well F-X1 exhibits highest values of porosity in the main reservoir unite (L1.2) about 25%, while the lowest rate was recorded in the well F-X3, since showed the lowest value of about 22% for the same unite as Table 2.

**Table 2.** Porosity and water saturation values of the Mishrif units in study wells

| Well ID | Reservior units | Effective Porosity (phie) | | | Water Saturation (Swe) | | |
|---|---|---|---|---|---|---|---|
| | | **Min.** | **Max.** | **Mean** | **Min.** | **Max.** | **Mean** |
| | U1.1 | 0 | 0.28 | 0.08 | 1 | 1 | 1 |
| | U1.2 | 0.11 | 0.30 | 0.26 | 1 | 1 | 1 |
| | U1.3 | 0 | 0.20 | 0.02 | 1 | 1 | 1 |
| | U2 | 0 | 0.30 | 0.17 | 1 | 1 | 1 |
| | Marl | 0 | 0.22 | 0.12 | 1 | 1 | 1 |
| F-X1 | M1.1 | 0 | 0.08 | 0.02 | 0.89 | 1 | 0.98 |
| | M1.2 | 0.04 | 0.25 | 0.17 | 0.50 | 0.84 | 0.63 |
| | M2 | 0 | 0.15 | 0.05 | 0.21 | 1 | 0.77 |
| | L1.1 | 0 | 0.22 | 0.12 | 0.28 | 1 | 0.50 |
| | L1.2 | 0 | 0.31 | 0.25 | 0.16 | 0.74 | 0.40 |
| | L2 | 0.12 | 0.30 | 0.22 | 0.59 | 1 | 0.95 |
| | | | | | | | |
| | U1.1 | 0.0083 | 0.22 | 0.06 | 1 | 1 | 1 |
| | U1.2 | 0.0793 | 0.20 | 0.16 | 1 | 1 | 1 |
| | U1.3 | 0 | 0.12 | 0.02 | 1 | 1 | 1 |
| | U2 | 0 | 0.26 | 0.16 | 1 | 1 | 1 |
| | Marl | 0 | 0.29 | 0.15 | 1 | 1 | 1 |
| F-X2 | M1.1 | 0 | 0.10 | 0.04 | 1 | 1 | 1 |
| | M1.2 | 0.09 | 0.23 | 0.19 | 0.48 | 0.811 | 0.60 |
| | M2 | 0.12 | 0.20 | 0.16 | 0.74 | 1 | 0.86 |
| | L1.1 | pinch out | | | pinch out | | |
| | L1.2 | 0.12 | 0.29 | 0.25 | 0.17 | 0.93 | 0.37 |
| | L2 | 0.07 | 0.26 | 0.17 | 0.69 | 1 | 1 |
| | | | | | | | |
| | U1.1 | 0 | 0.06 | 0.02 | 1 | 1 | 1 |
| | U1.2 | 0.03 | 0.15 | 0.11 | 1 | 1 | 1 |
| | U1.3 | 0 | 0.05 | 0.00 | 1 | 1 | 1 |
| | U2 | 0.02 | 0.20 | 0.11 | 1 | 1 | 1 |
| | Marl | 0 | 0.08 | 0.02 | 1 | 1 | 1 |
| F-X3 | M1.1 | 0 | 0 | 0 | 1 | 1 | 1 |
| | M1.2 | 0 | 0.19 | 0.14 | 0.06 | 1 | 0.29 |
| | M2 | 0.06 | 0.13 | 0.10 | 0 | 0.92 | 0.61 |
| | L1.1 | pinch out | | | pinch out | | |
| | L1.2 | 0.14 | 0.29 | 0.22 | 0 | 0.79 | 0.29 |
| | L2 | 0 | 0.17 | 0.09 | 0.80 | 1 | 0.99 |

## 5. 3. Water and Hydrocarbon Saturation

The total water saturation Swt and the effective water saturation Swe were computed using Archi formula in equations 8 and 9 respectively (Archie, 1942):

$$\mathrm{Swt} = [(\mathrm{a} \times \mathrm{Rw}) / (\mathrm{Rt} \times \emptyset \mathrm{t}^{\mathrm{m}})]^{1/\mathrm{n}}, \quad (8)$$

$$\mathrm{Swe} = [(\mathrm{a} \times \mathrm{Rw}) / (\mathrm{Rt} \times \emptyset e^{m})]^{1/\mathrm{n}}, \quad (9)$$

while of the invaded zone (Sxo) was calculated by using equation 9 through replacing of Rw with Rmf (resistivity of mud filtrate taken from headers of well logs), Rxo instead of Rxo (the invaded zone measured resistivity) and Øe with Øt (total porosity):

$$\mathrm{Sxo} = [(a \times Rmf) / (Rxo \times \emptyset t^{m})]^{1/\mathrm{n}} \quad (10)$$

where Rw = water formation resistivity which is calculated by well log analysis using cross and Pickett plots (Figs. 4, 5 and 6); a= factor of tortuosity; m= factor of cementation; n= exponent of saturation (Table 3).

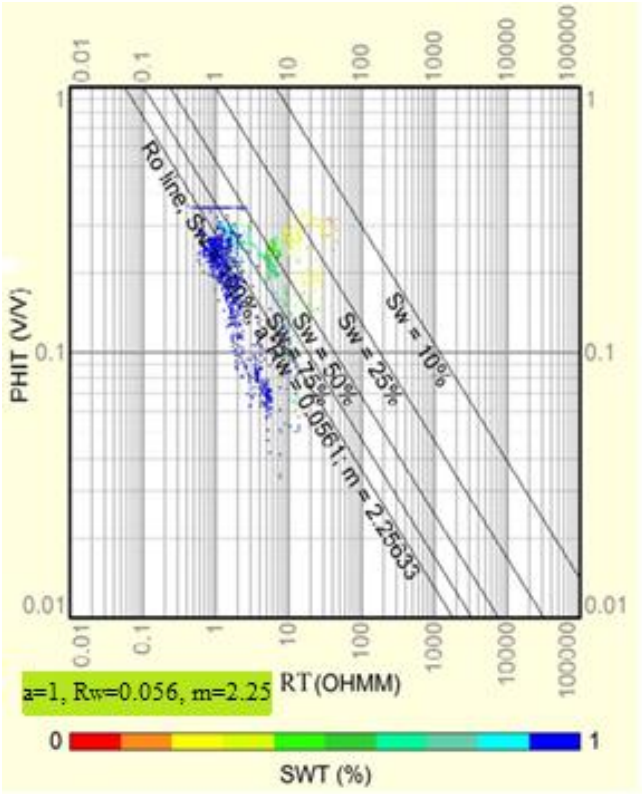


**Fig.4.** Picket plot analysis for well F-X1

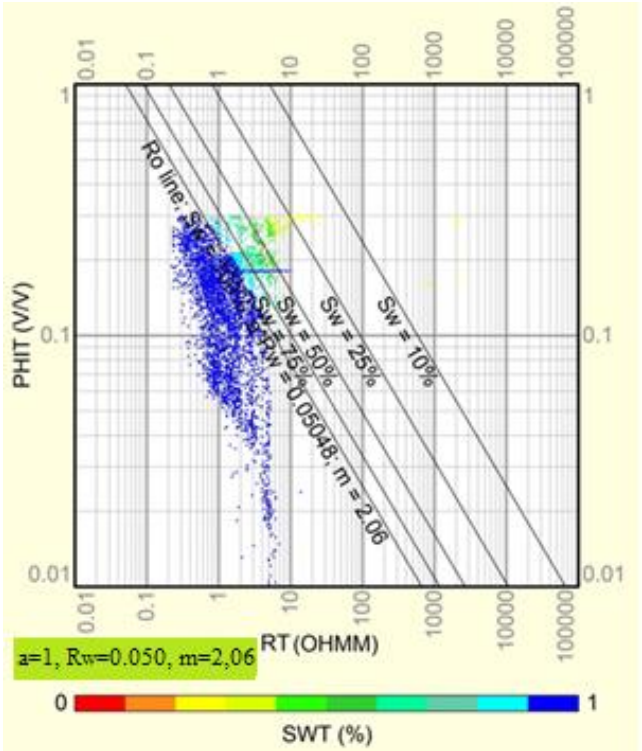


**Fig.5.** Picket plot analysis for well F-X2

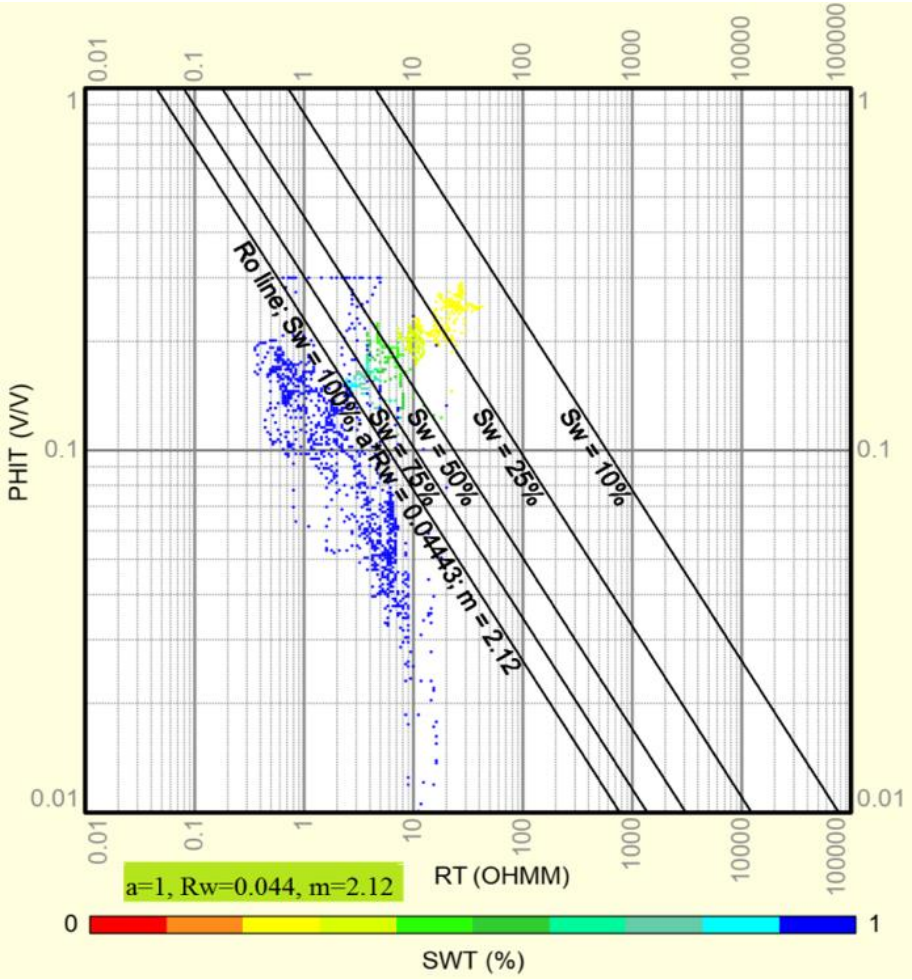


**Fig.6**. Picket plot analysis for well F-X3

**Table 3**. Represents the picket plot analysis of the study wells, where shows up the formation water resistivity (Rw) and Archi parameters: cementation factor (m), saturation exponent (n), tortuosity factor (a).

| Well ID | Rw | M | N | A |
|---|---|---|---|---|
| F-X1 | 0.056 | 2.25 | 2.07 | 1 |
| F-X2 | 0.050 | 2.06 | 2.02 | 1 |
| F-X3 | 0.044 | 2.12 | 2.10 | 1 |

The total saturation of hydrocarbons (Sht) was determined by equation of (Asquith et al., 2004):

$$\mathrm{Sht} = 1 - \mathrm{Swt} \qquad (11)$$

while, the saturation of moveable hydrocarbon (Shmov) was determined by the bellow equation:

$$\mathrm{Shmov} = \mathrm{Sxo} - Swt \qquad (12)$$

where Sht = total hydrocarbons saturation; Shmov = saturation of movable hydrocarbon; Sxo = invaded zone water saturation; Swt = uninvaded zone total water saturation.

### 5.4. Bulk volume (BV)

The uninvaded zone bulk volume of water (BVW) was calculated using the following equation:

$$BVW = Swt \times Øt \quad (13)$$

while, the bulk volume of hydrocarbons (Oil) can be calculated by the following equation:

$$Bvo = Sht \times Øt \quad (14)$$

where: Bvo = hydrocarbon's bulk volume; Sht = total saturation of hydrocarbon; Øt =total porosity.

## 6. Results and Discussions

The interpretation of computer processing (CPI) for studied wells (F-X1, F-X2 and F-X3) which represent that has been deduced using GEOLOG software (Figs.7, 8 and 9). Based on CPI results, the Mishrif Formation in F oil field could be subdivided into cap and reservoir units that are characterized by different Petrophysical properties. These include:

### 6.1. Cap Rocks

M1.1 and M2 are two cap units that have been identified at the middle part of the Mishrif Formation succession. The volume of shale values may be so high that the rocks of these units become marly. Unit M1.1 can have limited thickness (1.6m) as in well F-X3 (Fig.9). Both units show low values of effective porosity (PHIE) values. Water saturation, on the other hand, is very high. As a result, the volume of oil is low.

Marl is also a cap unit has been identified at the middle part (above M1.1 unit) of the Mishrif Formation succession. This unit show high values of total porosity (PHIT) and low of PHIE values. In the study wells, the thickness of the Marl unit ranges between 4 to 6 m (Figs.7, 8 and 9), which makes it a good insulation layer in the upper part of the first reservoir unit M1.2.

### 6.2. Reservoir Units

Reservoir units of the Mishrif Formation with high quality have common petrophysical properties, most notably high effective porosity and low water saturation. The lithology of these units is clean limestone characterized by low gamma ray log response. These properties are distinguished in units M1.2, L1.1, L1.2. The least quality reservoir units include U1.1, U1.2, U1.3, U2, and L2 due to their high-water saturation (Table 2).

#### *6.2.1. Unit U1.1*

This unit is located at the uppermost part of the Mishrif Formation overlain by the Khasib Formation. The transition from unit U1.1 to Khasib Formation shows sharp changes in the values of well logs due to the unconformable occurrence of shale rocks of the Khasib Formation above the limestone rocks of unit U1.1. The effect of dolomitization occurs in wells F-X2 and F-X3 (Figs.8 and 9). The low reservoir quality of this unit is attributed to low effective porosity and high-water saturation.

#### *6.2.2. Unit U1.2*

The unit U1.2 is confined between units U1.1 and U1.3. It is differentiated by higher total and effective porosity. However, this unit does not represent an important reservoir due to the high-water saturation. It can be traced in all wells and its thickness decreases significantly in well F-X1 (Fig.7). Dolomitization effect is prominent in wells F-X2 and F-X3 (Figs.8 and 9), so that the lithology is changed into dolomite.

*6.2.3. Unit U1.3*

The unit U1.3 shows a noticeable increase in the shale volume and a decrease in the porosity compared to the units U1.2 and U2. Dolomite in this unit appears less compared to unit U1.2. As with the unit U1.2, the unit U1.3 is totally saturated with water (Fig.7), which loses its reservoir quality.

*6.2.4. Unit U2*

The shale volume of unit U2 is largely reduces, which makes it easy to distinguish from the unit U1.3. This change is accompanied by a marked increase in porosity and water saturation (Fig.7). As is the case with the aforementioned units, the reservoir efficiency is low in this unit. The volume of dolomite is little in unit U2.

*6.2.5. Unit M1.2*

The M1.2 represents the uppermost reservoir unit that has good reservoir quality. It is capped by unit M1.1, and characterized by increase of effective porosity and decrease of water saturation associated with good oil volume as observed in well F-X3 (Fig.8). These reservoir properties decrease in other wells. The lithology of this unit is limestone with irregular changes in shale volume. The average of effective porosity and water saturation reach to 15% and 45%, respectively. Thickness of the unit decreases in wells F-X1 and F-X2 (Figs.7, 8).

*6.2.6. Unit L1.1*

This reservoir unit does not appear in all wells, which makes it less important. Furthermore, the unit is characterized by irregular changes in Petrophysical values (Fig.7). The average of effective porosity (PHIE) is 14%, and average of water saturation is 40%.

*6.2.7. Unit L1.2*

The L1.2 unit is considered the most important reservoir unit of the Mishrif Formation in the F oil field due to its large thickness, and high values of porosity and low water saturation. The average of PHIE is 26%, and average of water saturation reaches to 16%. The unit is capped by unit M2 where unit L1.1 is non-existent (Fig.8). The Petrophysical properties are gradually enhanced towards the top of the unit. Such trend in the Mishrif Formation was explained by (Mahdi et al., 2013; Mahdi and Aqrawi, 2017) as a result shallowing upward cycles that are accompanied by the increase of porosity resulted from dissolution.

*6.2.8 Unit L2*

The L2 represents the lowermost reservoir unit. Although this unit has a high porosity, it has low quality due to the high-water saturation. Limited increase of oil volume is observed at the uppermost part of the unit in well F-X1 (Fig.7). This unit has a large thickness and the lower boundary may not appear due to incomplete drilling to reach the lower boundary of the Mishrif Formation.

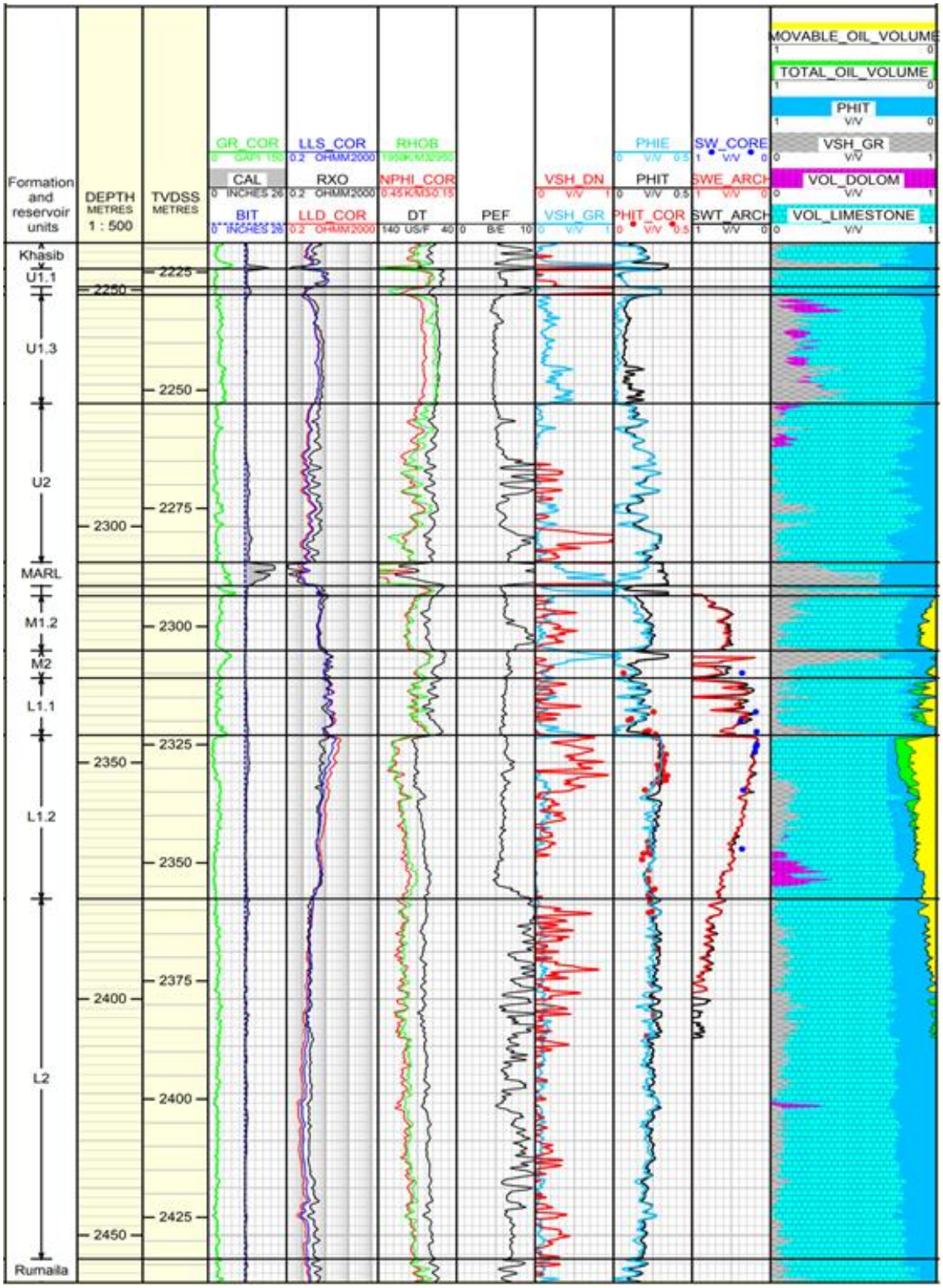


**Fig.7.** Computer Processes Interpretation (CPI) of well F-X1

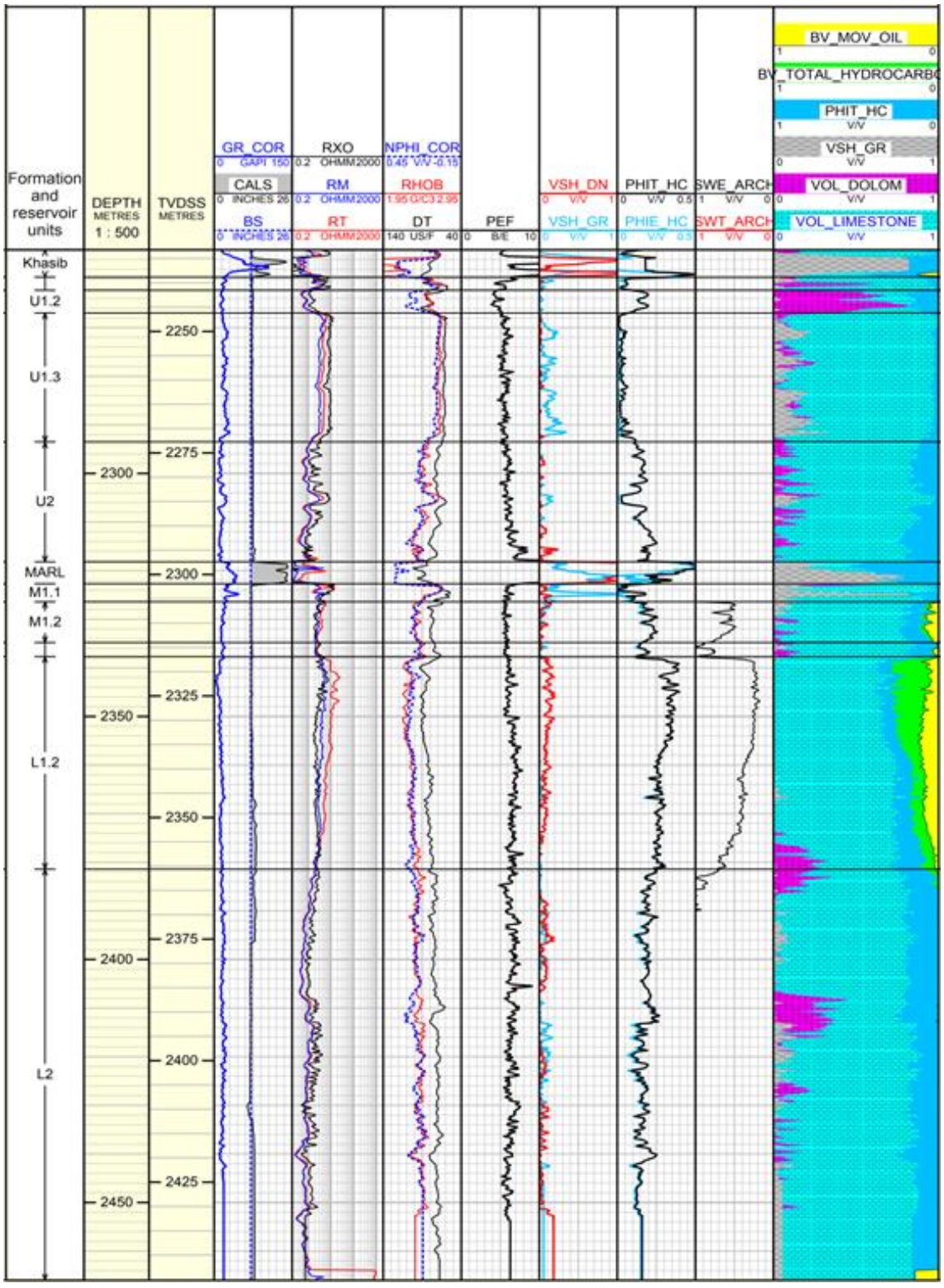


**Fig.8.** Computer Processes Interpretation (CPI) of well F-X2

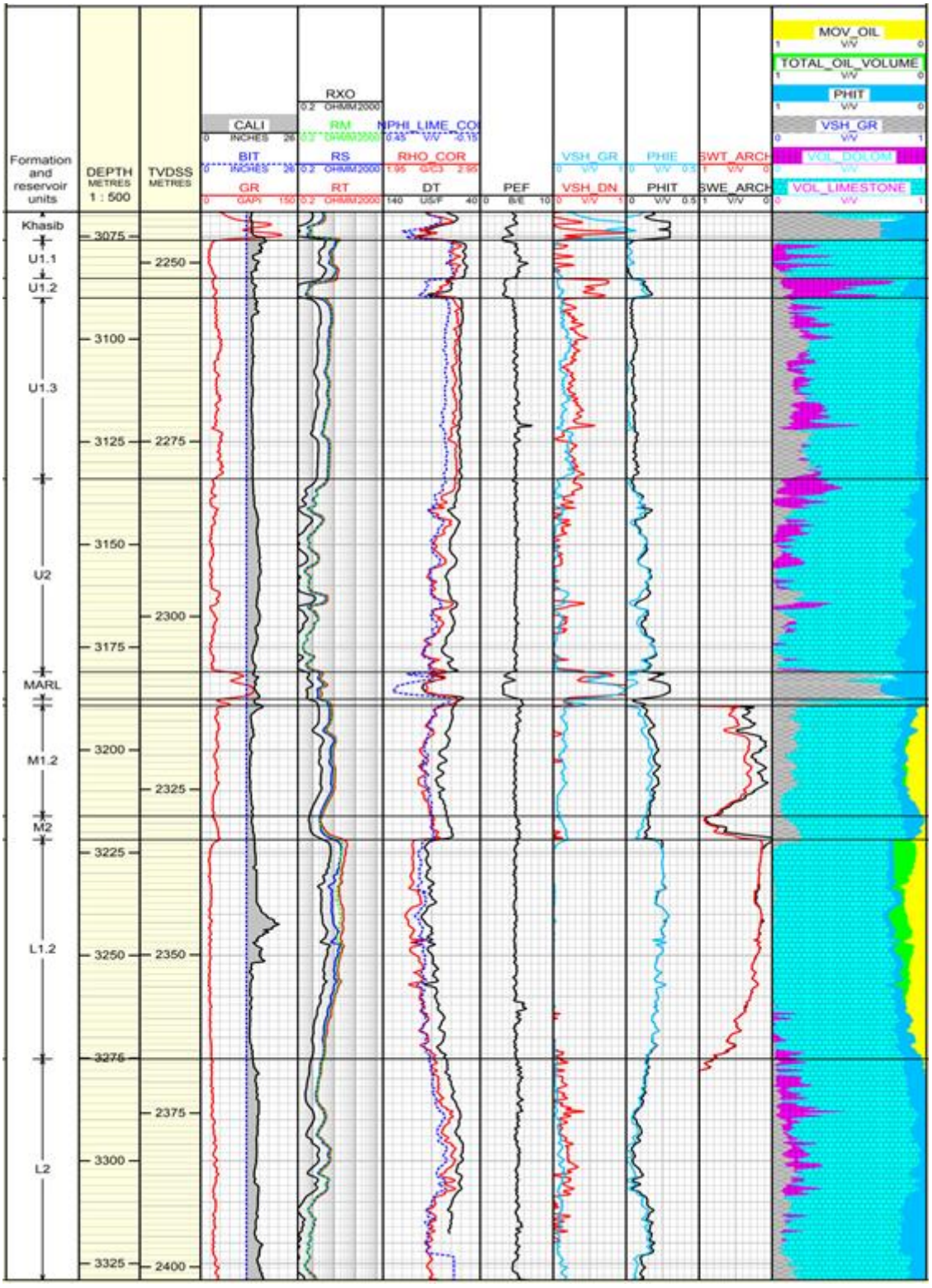


**Fig.9.** Computer Processes Interpretation (CPI) of well F-X3

## 7. Conclusions

The Mishrif Formation in the F oil field could be divided into several units of reservoir that differ in terms of a reservoir characteristics, depending on the results of the well logs analysis. Unit L1.2 is considered the most important due to the high effective porosity values and the decreasing water

saturation. Other units show lower quality reservoir properties due to increased water saturation as in units M1.2, L1.1 and L2. The cap units are characterized by increased shale volume and low effective porosity as in marl units and limestone units M1.1 and M2. The stratigraphic extent of the reservoir and the cap units can be traced in the study wells, except for the unit L1.1 which does not appear in the wells F-X2 and F-X3.

**Acknowledgements**

The authors are very grateful to the reviewers, Editor in Chief Prof. Dr. Salih M. Awadh, the Secretary of Journal Mr. Samir R. Hijab, and the Technical Editors for their great efforts and valuable comments

**References**

Abbas, L. K., Mahdi, T. A., 2020. Reservoir Modeling of the Mishrif Formation in Majnoon Oil Field, Southern Iraq. Iraqi Geological Journal, 89-101.

Al-Dulaimy, R. T., Al-Sheikhly, S., 2013. Biostratigraphy of the Mishrif Formation from well Amarah-1 southeastern Iraq. Iraqi Bulletin of Geology and Mining, 9(2), 1-14.

Al-Dulaimi, S. I., Al-Zaidy, A. A., Al-Sheikhly, S., 2013. 'The demise stage of rudist bearing Mishrif Formation (late Cenomanian–early Turonian), Southern Iraq. Iraqi Bulletin of Geology and Mining, 9(3), 1-20.

Al-Janaee, H. M., Al-shahwan, M. F., 2019. Estimation of porosity and permeability by using conventional logs and NMR Log in the Mishrif Formation, Buzurgan Oil Field. Journal of Petroleum Research and Studies, 9(3), 75-89.

Al-Mimar, H. S., Awadh, S. M., Al-Yaseri, A. A., Yaseen, Z. M., 2018. Sedimentary units-layering system and depositional model of the carbonate Mishrif reservoir in Rumaila oilfield, Southern Iraq. Modeling Earth Systems and Environment, Springer, 4(4), 1449-1465.

Al-Najm, F. M., Al-Shahwan, M. F., Al-Beyati, F. M., 2017. Petrophysical characteristics and reservoir modeling of Mishirf Formation at Noor Oil Field, South of Iraq. Journal of Petroleum Research and Studies, 7(1), 210-235.

Aqrawi, A. A. M., Goff, J. C., Horbury, A. D., Sadooni, F. N., 2010 The Petroleum Geology of Iraq. Scientific Press, Bucks, UK.

Archie, G. E., 1942. The electrical resistivity log as an aid in determining some reservoir characteristics', Transactions of the AIME. OnePetro, 146(01), 54-62.

Asquith, G. B., Krygowski, D., Gibson, C. R., 2004 Basic well log analysis. American Association of Petroleum Geologists Tulsa.

Awadeesian, A.M., Awadh, S.M., Al-Dabbas, M.A., Al-Maliki, M.M., Al-Jawad, S.N., Hussein, A.K.S., 2019. A modified water injection technique to improve oil recovery: Mishrif carbonate reservoirs in southern Iraq oil fields, case study. The Iraqi Geological Journal,125-146.

Awadeesian, A. M. R., Al-Jawad, S. N. A., Awadh, S. M., Al-Maliki, M. M., 2018. Chronostratigraphically based reservoir model for Cenomanian Carbonates, Southeastern Iraq Oilfields. Iraqi Geological Journal, 1-27.

Awadh, S. M., Al-Mimar, H. S., Al-Yaseri, A. A., 2018. Salinity mapping model and brine chemistry of Mishrif reservoir in Basrah oilfields, Southern Iraq. Arabian Journal of Geosciences. Springer, 11(18), 1-12.

Dresser, A., 1979. Log interpretation charts: Houston, Dresser Industries, Inc, 107.

Handhal, A. M., Al-Shahwan, M. F., 2014. Evaluation of microfacies of Mishrif Formation in Nassyria Oil Filed, south of Iraq. Journal of Basrah Researches (Sciences). Basrah University, 40(2B).

Handhal, A. M., Chafeet, H. A., Dahham, N. A., 2020. Microfacies, depositional environments and diagenetic processes of the Mishrif and Yamama formations at Faiha and Sindibad oilfields, south Iraq. Iraqi Bulletin of Geology and Mining, 16(2), 51-74.

Ismail, M. J., Ettensohn, F. R., Handhal, A. M., Al-Abadi, A., 2021.Facies analysis of the Middle Cretaceous Mishrif Formation in southern Iraq borehole image logs and core thin-sections as a tool, Marine and Petroleum Geology. Elsevier, 133, 105324.

Mahdi, T. A., Aqrawi, A. A. M., 2017. Role of facies diversity and cyclicity on the reservoir quality of the mid-Cretaceous Mishrif Formation in the southern Mesopotamian Basin, Iraq. Geological Society, 435(1), 85–105.

Mahdi, T. A., Aqrawi, A. A. M., Horbury, A. D.Sherwani, G. H., 2013. Sedimentological characterization of the mid-Cretaceous Mishrif reservoir in southern Mesopotamian Basin, Iraq. GeoArabia. Gulf PetroLink, 18(1), 139-174.

Mohammed, M. J., Mahdi, T. A., 2019. Petrophysical characterizations of Mishrif Formation in Selected Wells of Tuba Oil Field, Southern Iraq, Iraqi Journal of Science, 516–527.

Oil Exploration Company, 1995. An integrated geological and evaluation study of Gharraf oil field.

Oil Exploration Company, 2010. Geophysical - geological - assessment study of the Gharraf field with 3D technology.

Schlumberger, 1974. Log Interpretation, Vol. II-Applications', Ltd., New York.

Schlumberger, 1998. Cased Hole Log Interpretation Principles/ Applications Houston, Schlumberger Wireline and Testing, 198.

South Oil Company (S.O.C), 1991.Facies reservoir study of Mishrif Formation in Gharraf oil field. Basrah, Iraq.

Tiab, D., Donaldson, E. C., 1996. Theory and practice of measuring reservoir rock and fluid transport properties. Gulf Publishing Company, Houston, TX, 4, 200.

Wyllie, M. R. J., Gregory, A. R., Gardner, G. H. F., 1958. An experimental investigation of factors affecting elastic wave velocities in porous media. Geophysics. Society of Exploration Geophysicists, 23(3), 459-493.